

Strain monitoring of reinforced concrete with OTDR-based FBG interrogation technique

Anton V. Dyshlyuk^{*1,2}, Natalia V. Makarova^{1,2},
Oleg B. Vitrik^{1,2}, Yuri N. Kulchin^{1,2} and Sergey A. Babin³

¹Institute of Automation and Control Processes FEB RAS, 5 Radio Str., 690041, Vladivostok, Russia

²Far Eastern Federal University, 8, Sukhanova Str., 690091, Vladivostok, Russia

³Institute of Automation and Electrometry SB RAS, Academician Koptug ave. 1, 630090, Novosibirsk, Russia

(Received October 25, 2016, Revised June 26, 2017, Accepted June 28, 2017)

Abstract. An experimental study is presented of the application of fiber Bragg grating (FBG) interrogation method based on optical time-domain reflectometry (OTDR) to monitoring strain in bent reinforced concrete beams. The results obtained with the OTDR-based method are shown to agree well with the direct spectral measurements. Strain sensitivity, resolution and measurement range amounted to 0.0028 dB/ μ strain; 30 μ strain; 4000 μ strain, correspondingly. Significant differences are observed in surface and inner deformations of the test beams which can be attributed to different mechanical properties of concrete and steel reinforcement. The prospects of using OTDR-based FBG interrogation technique in real-life applications are discussed.

Keywords: OTDR; FBG; strain; reinforced concrete; structural health monitoring

1. Introduction

Nowadays, rapid development of civil infrastructure along with the introduction of increasingly stringent safety standards calls for state-of-the-art structural health monitoring (SHM) systems transforming conventional engineering constructions into smart structures. Such systems enable precise measurements of strains and stresses, temperatures, linear and angular displacements of structural elements, etc. (see e.g., Myung *et al.* 2014, Li *et al.* 2010, Balageas *et al.* 2006, Chang *et al.* 2003). By processing and analyzing the data collected it becomes possible to make predictions about the development of deformation processes and thus prevent or drastically reduce the likelihood of structural failures.

Among various SHM techniques and devices such as visual inspection, acoustic and radiographic methods, mechanical, electrical and other types of sensors it is fiber optic sensors (FOS) that appear particularly promising due to their inherent advantages such as electromagnetic noise immunity, environmental ruggedness, very small size and weight, longevity and sensitivity to a wide range of physical quantities (see e.g., López-Higuera *et al.* 2011, Kesavan *et al.* 2005, Merzbacher *et al.* 2013, Kersey and Friebale 1996, Kulchin *et al.* 1993, Kulchin *et al.* 1997, Bykovskii *et al.* 1990).

The most widely used FOS in structural health monitoring are those based on fiber Bragg gratings (FBG) (Pang *et al.* 2013, Talebinejad *et al.* 2009, Majumder *et al.*

2008, Baier *et al.* 2008). An FBG represents a short section of single-mode optical fiber with a periodically modulated refractive index (typical modulation length and period are on the order of a few mm and \sim 500 nm, correspondingly). Such a structure can be inscribed in the fiber by photo-induced recording in a variety of interference-based optical schemes (Vasil'ev *et al.* 2005). As broad-band radiation propagates along the fiber it reflects from the Bragg grating in a narrow spectral range centered at the resonant wavelength of the grating. When an FBG is subjected to mechanical strain or temperature variation its resonant wavelength is shifted by a typical amount of 0.01 nm per 1°C or 0.001 nm per 1 μ strain (Vasil'ev *et al.* 2005). Thus, by performing spectral measurements of the light transmitted or reflected from an FBG it is possible to determine its strain and/or temperature and hence those of the structural element it is attached to. One of the major advantages of FBG-sensors especially in SHM applications involving large scale structures is the ability to multiplex signals of many sensors recorded in a single fiber optic line (see e.g., Majumder *et al.* 2008, Baier *et al.* 2008, Vasil'ev *et al.* 2005).

Nonetheless, despite their numerous advantages widespread use of FBG-based sensors and measuring systems in SHM applications is somewhat hindered by the relatively high costs of optical equipment required for spectral demultiplexing of FBG signals, which is one of the most common approaches to their interrogation. This justifies the development and implementation of simpler and cheaper FBG interrogation schemes. One way to achieve this goal is to switch from spectrally-modulated to intensity-modulated detection regime by converting the resonant wavelength shift of the grating into light intensity variation that can be

*Corresponding author, Ph.D.
E-mail: anton_dys@iacp.dvo.ru

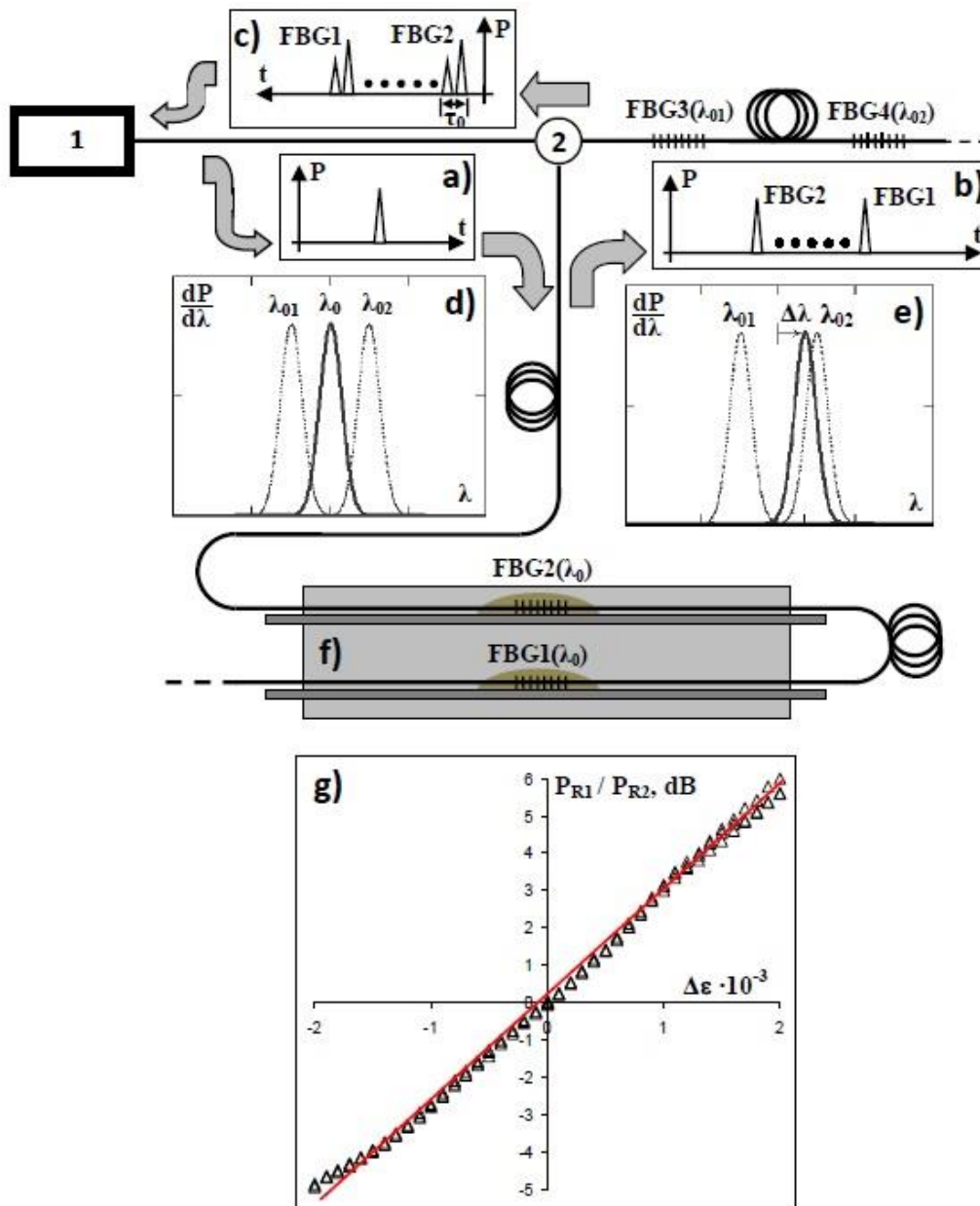


Fig. 1 Schematic of the measuring system: 1 – fiber optic relectometer, 2 – fiber optic circulator, FBG1 and FBG2 – sensing Bragg gratings, FBG3 and FBG4 – reference Bragg gratings. In the insets: (a) – probing pulse generated by OTDR, (b) - sequence of two signal pulses reflected from the FBG-sensors, (c) – a sequence of four pulses after multiple reflections of the signal pulses from the reference FBGs, (d) – reflection spectrum of an FBG sensor (at λ_0) and reference FBGs (at λ_{01} and λ_{02}) with no strain applied to the sensor, (e) – reflection spectra of an FBG sensor and reference FBGs with some strain applied to the sensor, (f) – schematic drawing of the test beam with FBG sensors on its reinforcing rods and (g) – reflectometrically measured signal from an FBG sensor vs. its relative elongation

measured directly by an optical power meter. Conventional optical time domain reflectometry (OTDR) can be employed in this case to enable interrogation of multiple FBGs within one line (see e.g., Carlos Guedes Valente *et al.* 2003, Zhang *et al.* 2003, Kulchin *et al.* 2008, 2011). OTDR-based method makes it possible to interrogate up to several hundred sensors recorded in a single fiber optic line while at the same time reducing the costs associated with implementing FBG-based measuring systems by making use of relatively inexpensive reflectometric equipment

instead of optical spectrum analyzers (Kulchin *et al.* 2011).

OTDR-based FBG interrogation principle was investigated extensively but, to the best of our knowledge, its practical utilization for strain monitoring of building elements has not yet been studied in detail experimentally. Thus, the purpose of the paper is to demonstrate application of OTDR-based FBG interrogation technique to monitoring strain in reinforced concrete beams under bend tests.

2. OTDR-based FBG interrogation technique

A schematic of the measuring system is shown in Fig. 1.

It consists of a standard fiber optic time domain reflectometer (OTDR) ANDO AQ7250 (1), a signal arm with two FBG sensors (FBG1 and FBG2), and an arm with two reference FBGs (FBG3 and FBG4). The reference arm serves the purpose of converting spectrally modulated signals of FBG sensors into intensity modulated as well as providing power reference to make the measuring system immune to light intensity fluctuations (Kulchin *et al.* 2008, 2011). The FBG sensors are embedded into test beams so that when the beam is bent they turn out to be in its tensile and compressed zones (Fig. 1(f)). The details of fabricating the beams and positioning the sensors are discussed below. Both the sensing and reference Bragg gratings are recorded in a SMF-28-type single mode optical fiber by a standard holographic technique.

The operation principle of the system is as follows. A probing pulse generated by OTDR 1 (Fig. 1(a)) passes through fiber optic circulator 2 into the signal arm where it is successively reflected from FBG-sensors FBG2 and FBG1 (Fig. 1(b)). Each of the reflected pulses is then again reflected from the two reference FBGs (FBG3 and FBG4) thus giving rise to two new pulses separated by a short time delay τ_0 (Fig. 1(c)) that are received by OTDR. Each pair of pulses corresponding to a single FBG-sensor carries information about its strain. The initial resonant wavelength of the FBG-sensors (λ_0) is chosen to be right in between those of the reference FBGs (λ_{01} and λ_{02}), so that when no strain is applied to a sensor the overlap of its reflection spectrum with that of each reference FBGs is the same, leading to equal powers of the pulses in the corresponding pair: $P_{R1} = P_{R2}$. When the sensor's resonant wavelength is shifted by $\Delta\lambda$ due to the applied strain the power carried by one the pulses increases while that of the other decreases. The measured signal defined as P_{R1} / P_{R2} does not depend directly on the power of the original probing pulse thus making the system immune to undesired intensity variations such as OTDR laser power fluctuations or bend-induced losses in optical fibers (Kulchin *et al.* 2008, 2011).

Since the spectrum of OTDR's semiconductor laser is not continuous but consists of discrete longitudinal modes, to ensure a monotonous dependence of the measured signal on $\Delta\lambda$, the FWHM of FBG reflection spectrum (A) must exceed the inter-modal spectral gap ($d\lambda$) (Kulchin *et al.* 2008, 2011). For the OTDR used in the present work (ANDO AQ7250) $d\lambda$ is about 0.7 nm, so A was chosen to be 1 nm. The resonant wavelengths of the Bragg gratings were selected to be within the spectrum of OTDR laser near 1550 nm: reference FBGs - $\lambda_{01} = 1555$ nm, $\lambda_{02} = 1558$ nm; FBG sensors - $\lambda_0 = 1556.5$ nm. We used weakly reflecting gratings for FBG sensors (2% reflectivity at the resonant wavelength), and moderately (30%) reflecting gratings for reference FBGs.

3. Experimental details

During preliminary tests of the system before attaching the sensors to the test beam reinforcing cage we measured the dependence of an FBG sensor signal on its relative elongation (Fig. 1(g)). As can be seen from the figure, the chosen parameters of the sensing and reference FBGs correspond to the optimal measurement conditions for this dependence is very near to linear. Strain sensitivity amounted to 0.0028 dB / μ strain (spectral sensitivity is 4 dB per 1 nm of $\Delta\lambda$) within the measurement range of about 4000 μ strain. Resolution of power loss measurement by OTDR has a typical value of 0.03 dB per every 1 dB of the loss being measured. In the proposed configuration two peaks in the OTDR trace correspond to each of the interrogated sensors, with one of them growing and the other diminishing in magnitude when FBG sensor's resonant wavelength is shifted due to the applied strain. Therefore with ~ 10 dB of the total range of the measured power ratio P_{R1} / P_{R2} (see Fig. 1(g)) we can take roughly ~ 5 dB as the maximum measured loss and 0.15 dB the maximum uncertainty of measuring P_{R1} / P_{R2} . The average value of this uncertainty in the elongation range of ~ 4000 μ strain is thus $0.5 \cdot (0.03 + 0.15) = 0.09$ dB which translates into an average strain resolution of ~ 30 μ strain. This figure is approximately an order of magnitude larger than that achievable with more expensive spectrally interrogated FBG sensor systems but still deemed sufficient for many applications in structural health monitoring.

After testing the system, FBG sensors were attached with cyanoacrylate cement to steel reinforcing rods of class B-I (1 m in length and 5 mm in diameter) and calibrated by using a universal testing machine Shimadzu AGS-X 10 kN (Fig. 2(a)) and a contact extensometer (Fig. 2(b)). From the calibration tests we obtained the dependences of the FBG sensor signals on the relative elongation of the rods in the elastic range. A typical calibration dependence measured several times for one of the sensors is shown in Fig. 2(c). As one can see, it reproduces itself within an error of ~ 0.1 dB and is linear in the range of elastic deformations of the rod, which suggest that the strain of the rod is directly carried over to the optical fiber with FBG. The measurements were performed in a 1500- μ strain deformation range with a 4-dB dynamic range of the registered signal.

After calibration tests, the rods with FBG sensors were used to make reinforcing cage for the test beams. A total of two beams (B-1 and B-2) sized 0.04 \times 0.1 \times 0.9 m were made out of plain concrete with strength class B15. The reinforcing cage was placed in the forms so that one of the FBG sensors (FBG1) would be in the tensile zone while the other one (FBG2) - in the compressed zone of the bent beam.

After 28 days of curing 30-mm-long resistance strain gauges (SG1 and SG2) were attached to the surface of the test beams at the same levels with FBG1 and FBG2 sensors. The details about the test beams including dimensions, reinforcing cage, sensor placement, loading applied during the bend tests, and the photo of the forms for their fabrication are presented in Fig. 3.

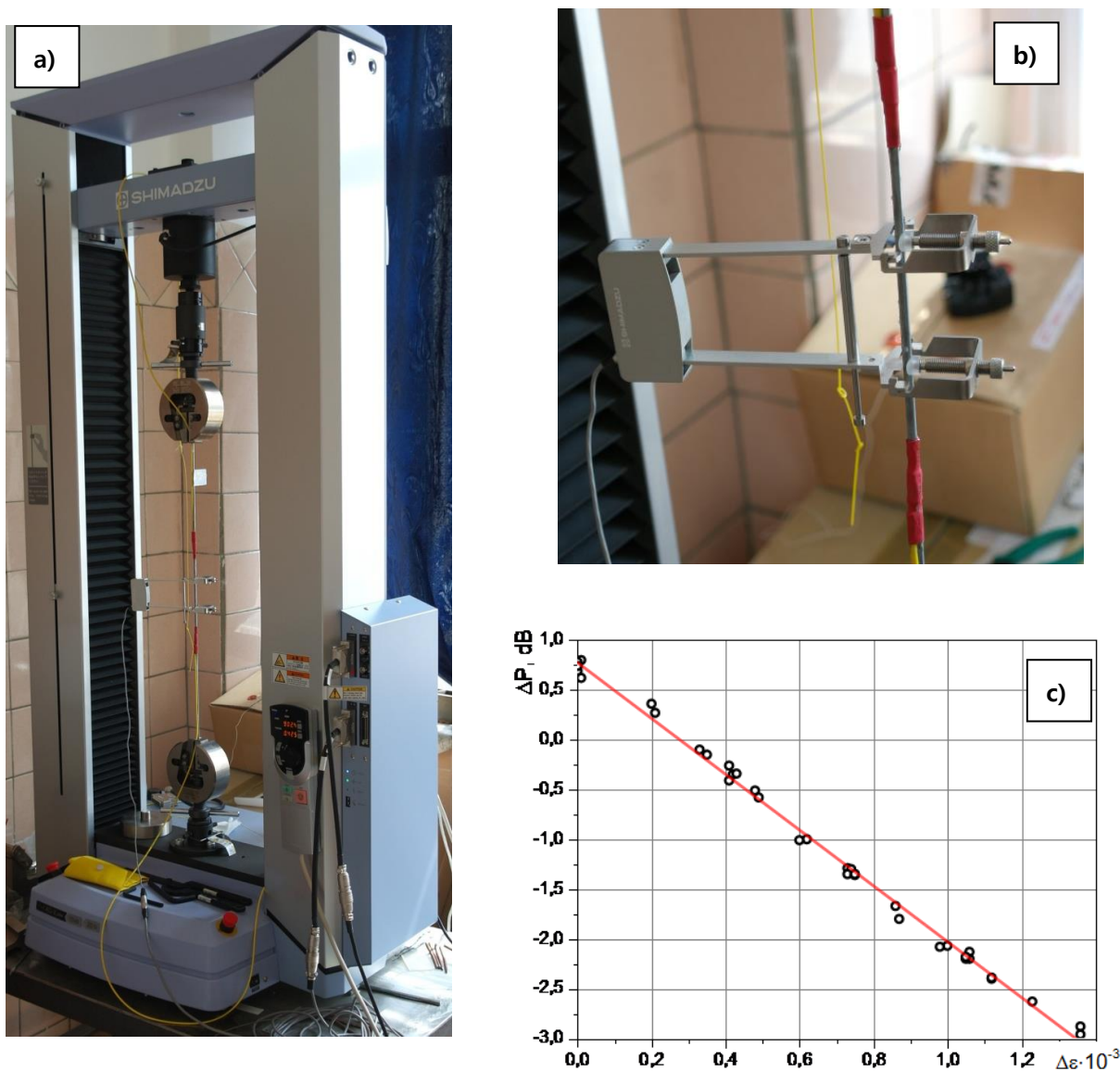


Fig. 2 Calibration tests of the sensitive elements: (a) – photo of the setup for calibration tests and (b) – using a contact extensometer for direct measurement of the reinforcing rod elongation and (c) – a typical calibration dependence of the measured signal on the relative elongation of the reinforcing rod

Four-point bend tests of the beams were carried out using Shimadzu AGS-X 10 kN universal testing machine. The applied load P was increased in $50 \div 200\text{N}$ steps and the sensor signals were registered after 1 minute of keeping the beam under constant load in each step. The rate of applying load during testing beams B-1 and B-2 amounted to 1 MPa/s and 0.2 MPa/s , correspondingly. The deflection of the beam with applied load was measured by a conventional deflectometer (Fig. 4).

When testing beam B-1 the readings of the FBG-sensors were obtained both by the reflectometric method and by direct spectral measurements using a broad-band ASE light source Thorlabs ASE570 and optical spectrum analyzer (OSA) Yokogawa 6370B. The strain gauge signals were registered by ADC-DAC module ZET210.

4. Bend test results

Fig. 5 shows the results of measuring strain of the reinforcing rods (sensors FBG1 and FBG2) and concrete (sensors SG1 and SG2) versus applied load during testing beam B-1. As seen from the figure, according to the respective positions of FBG1 and FBG2 in the tensile and compressed zones of the beam, the signal from the first one grows with loading while that from the second goes down. The beam destructed at $P=1.6 \text{ kN}$, with the failure being of brittle character as a main crack rapidly developed from the tensile zone into the compressed one.

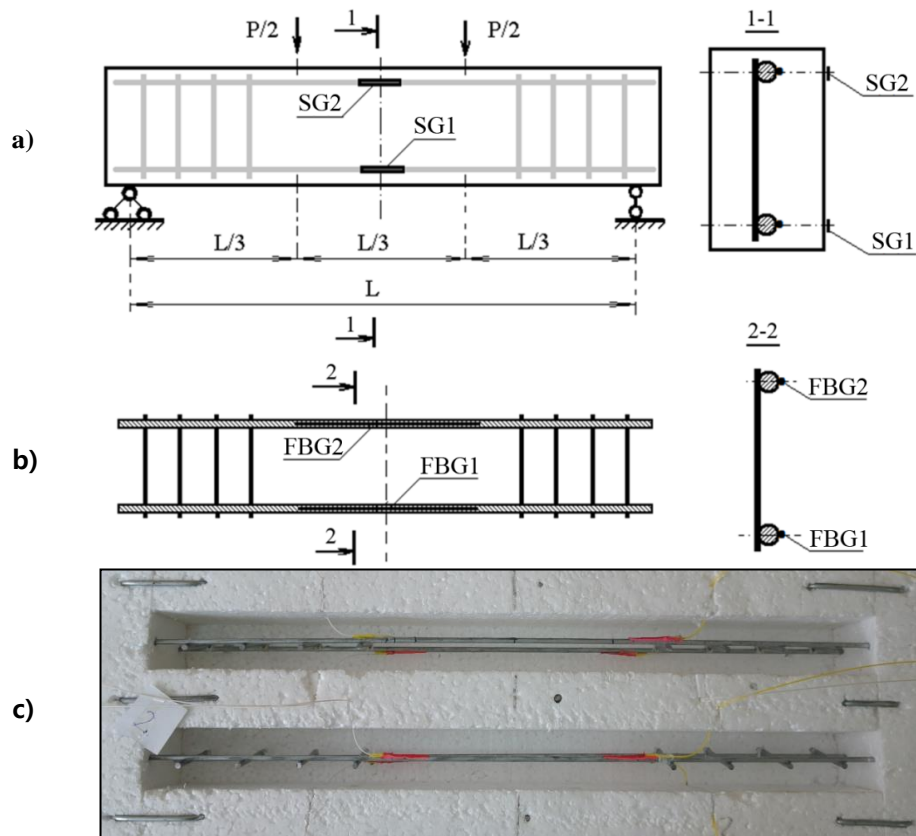
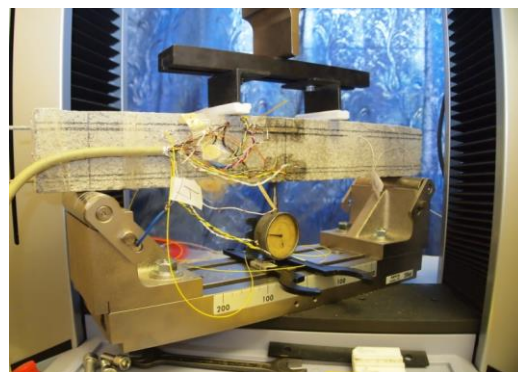
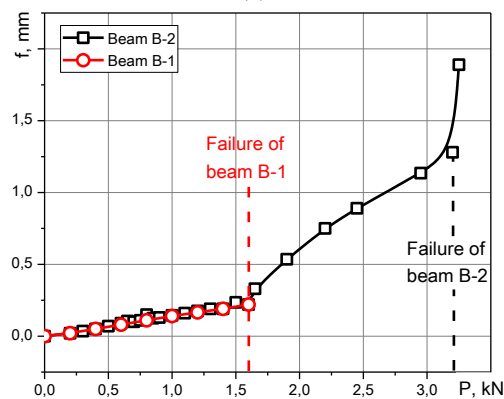


Fig. 3 Drawings of the test beams (a), (b) and photo of the forms for their fabrication (c)



(a)



(b)

Fig. 4 Photo of the beam during deformation tests (a) and measured deflection of beams B-1 and B-2 versus the applied load (b)

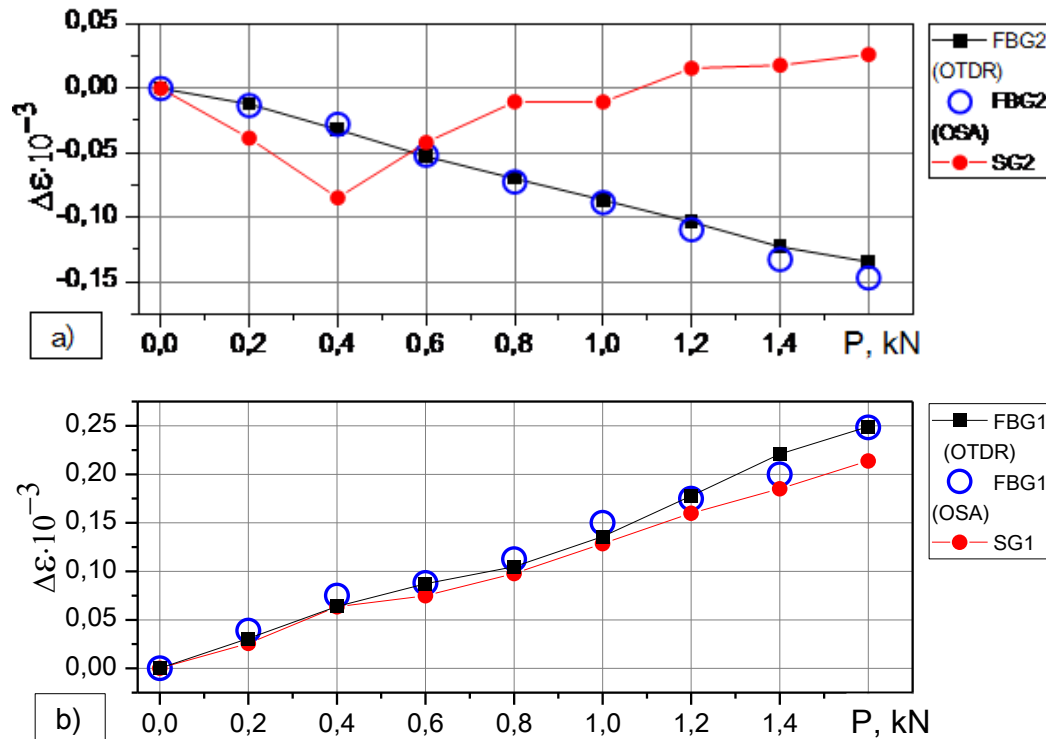


Fig. 5 Bend test results for beam B-1: (a) – readings of the sensors in the compressed zone of the beam (FBG2, SG2) and (b) – readings of the sensors in the tensile zone of the beam (FBG1, SG1) versus applied load. FBG sensor signals were registered both by the reflectometric method and direct spectral measurements

Up to the moment of failure the deformation of the reinforcing rods was in elastic stage so that the readings of the FBG sensors are essentially straight lines. As can also be seen from the figure, the FBG sensor signals obtained with the reflectometric method and direct spectral measurements are in close agreement. Therefore, when testing beam B-2 we used only the OTDR-based method.

The readings of the strain gauge SG1 in the tensile zone of the beam reproduce with a slight lag those of FBG1. However the signal from SG2 in the compressed zone of the beam is drastically different from that of FBG2. This can be explained by a change of sign of deformation increments in the near-surface layer of the beam due to volume micro-cracking of the compressed concrete.

The results of testing beam B-2 are shown in Fig. 6. The beam destructed at $P=3.25$ kN with the failure being of plastic character. At $P=0.5$ kN concrete strains in the tensile zone of the beam reached their limits and cracks began to open up leading to strain relaxation in the near-surface layer. This is evident from the signal of SG1 exhibiting a characteristic jump followed by zero readings. At the same time the reinforcing rods both in the tensile and compressed zones remained in the elastic deformation stage although the FBG sensor signals do contain jumps and other features indicative of crack formation.

The failure of the beam started with stresses in the compressed zone of the beam reaching their limits at $P\sim 2.2$ kN. As follows from the readings of SG2, just as was the case with beam B-1, the bending of the beam was accompanied by the sign change of surficial deformation

increments due to volume micro-cracking of the compressed concrete. At the same time the compression of the upper reinforcing rod progressed as is evidenced by the signal from FBG2. The final breakage of the beam resulted from a main crack developing from the compressed zone into the tensile one and splitting the beam into two parts connected with still working reinforcement.

The differences in the test results for beams B-1 and B-2 can be explained by different rates of applying load as well as by specific details of microscopic structure of the beams, random inhomogeneities in the concrete and other uncontrollable factors.

Based on the results obtained we can draw the conclusion that the readings of the FBG sensors on the reinforcing rods and the strain gauges on the concrete surface differ because of peculiarities of reinforced concrete as a complex structural material. At initial stages of deformation strain in the concrete normally exceeds that in the reinforcement owing to their different mechanical properties. On the other hand, as cracks start to appear in the tensile zone of the beam deformations in the concrete tend to relax because of internal stresses carrying over to the reinforcement. Thus, measuring concrete deformations in near-surface layers does not provide adequate information on the stress-strain state of the reinforcement. It is, however, of primary interest in structural health monitoring because a deformation can be considered a structural failure when the strain in reinforcement has reached the yield point.

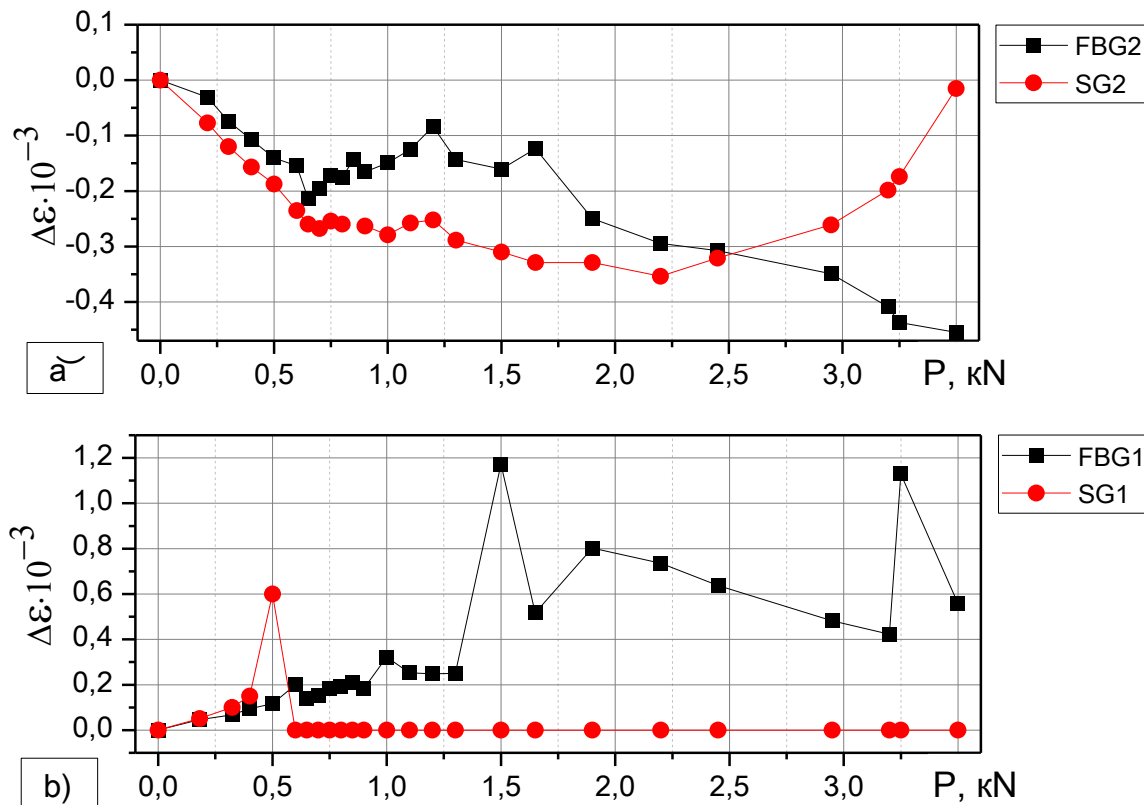


Fig. 6 Bend test results for beam B-2: (a) – readings of the sensors in the compressed zone of the beam (FBG2, SG2) and (b) – readings of the sensors in the tensile zone of the beam (FBG1, SG1) versus applied load

Thus, integrating strain sensors directly into reinforcement appears a key element of health monitoring of reinforced concrete structures. Electrical resistance strain gauges are not particularly suitable for that purpose owing to their susceptibility to electromagnetic interference and rigid requirement on hydro insulation and mechanical protection of both sensitive elements and lead wires. However, FBG-based fiber optic strain sensors are immune to electromagnetic noise and tolerant to harsh environments so integrating them into the reinforcement of structural elements seems appropriate and advantageous. Furthermore using OTDR-based method for their interrogation makes it possible to drive down the costs of FBG-based measuring systems thus widening their application range.

5. Conclusions

We have presented an experimental study of application of the OTDR-based FBG interrogation method for strain monitoring of reinforced concrete beams under bend tests. It has been shown that the results of measuring strain of FBG sensors on reinforcing rods of the test beams obtained with OTDR-based method are in close agreement with the direct spectral measurements. Experimentally achieved strain sensitivity, resolution and measurement range are $0.0028 \text{ dB}/\mu\text{strain}$, $30 \mu\text{strain}$, and $4000 \mu\text{strain}$, correspondingly.

In the course of bend tests substantial differences were observed in the character of near-surface and inner

deformations of the test beams which can be attributed to different structural behavior of reinforcing steel and concrete. Thus, to effectively assess the inner stress-strain state of reinforced concrete structures sensors need to be integrated into their reinforcing cage. FBG-based fiber optic sensors appear particularly suitable for this purpose while utilizing the reflectometric method for their interrogation promises considerable reduction in the costs of FBG-based monitoring systems.

Acknowledgements

The research was partially supported by RFBR (16-32-00384_мол_а) and FASO of Russia (the Far East Program, grants 0262-2015-0087, 0262-2015-0058, 0262-2015-0060).

References

- Baier, H., Mueller, U.C. and Rapp, S. (2008), "Fiber optic sensor networks in smart structures", *Proceedings of the 15th International Symposium on: Smart Structures and Materials & Nondestructive Evaluation and Health Monitoring*, International Society for Optics and Photonics.
- Balageas, D., Fritzen, C.P. and Güemes, A. (Eds.) (2006), *Structural health monitoring*, **493**, London: ISTE.
- Bykovskii, Y.A., Vitrik, O.B. and Kulchin, Y.N. (1990), "Amplitude spatial filtering in the processing of signals from a single-fiber multimode interferometer", *Soviet J. Quantum*

- Electron.*, **20**(10), 1288.
- Carlos Guedes Valente, L., Braga, A.M.B., Santanna Ribeiro, A., Dias Regazzi, R., Ecke, W., Chojetzki, C. and Willsch, R. (2003), "Combined time and wavelength multiplexing technique of optical fiber grating sensor arrays using commercial OTDR equipment", *IEEE Sens. J.*, **3**(1), 31-35.
- Chang, P.C., Flatau, A. and Liu, S.C. (2003), "Review paper: health monitoring of civil infrastructure", *Struct. Health Monit.*, **2**(3), 257-267.
- Kesavan, K., Ravisankar, K., Parivallal, S. and Sreeshylam, P. (2005), "Applications of fiber optic sensors for structural health monitoring", *Smart Struct. Syst.*, **1**(4), 355-368.
- Kulchin, Y.N., Vitrik, O.B., Kirichenko, O.V. and Petrov, Y.S. (1993), "Multidimensional signal processing using a fiber-optic distributed measuring network", *Kvantovaya Elektronika Moscow*, **20**, 513-516.
- Kulchin, Y.N., Vitrik, O.B., Kirichenko, O.V., Kamenev, O.T., Petrov, Y.S. and Maksaev, O.G. (1997), "Method of single-fiber multimode interferometer speckle-signal processing", *Opt. Eng.*, **36**(5), 1494-1499.
- Kulchin, Y. N., Vitrik, O. B., Dyshlyuk, A. V., Shalagin, A. M., Babin, S.A., Shelemba, I.S. and Vlasov, A.A. (2008), "Combined time-wavelength interrogation of fiber-Bragg gratings based on an optical time-domain reflectometry", *Laser Phys.*, **18**(11), 1301-1304.
- Kulchin, Y.N., Vitrik, O.B., Dyshlyuk, A.V., Shalagin, A.M., Babin, S.A. and Nemov, I.N. (2011), "Differential reflectometry of FBG sensors in the wide spectral range", *Laser Phys.*, **21**(2), 304-307.
- Kulchin, Y.N., Vitrik, O.B., Dyshlyuk, A.V., Shalagin, A.M., Babin, S.A. and Nemov, I.N. (2011), "Differential multiplexing of fiber Bragg gratings by means of optical time domain refractometry", *Measurement Techniques*, **54**(2), 170-174.
- Li, P., Gu, H., Song, G., Zheng, R. and Mo, Y.L. (2010), "Concrete structural health monitoring using piezoceramic-based wireless sensor networks", *Smart Struct. Syst.*, **6**(5-6), 731-748.
- López-Higuera, J.M., Cobo, L.R., Incera, A.Q. and Cobo, A. (2011), "Fiber optic sensors in structural health monitoring", *J. Lightwave Technol.*, **29**(4), 587-608.
- Merzbacher, C.I., Kersey, A.D. and Friebele, E.J. (1996), "Fiber optic sensors in concrete structures: a review", *Smart Mater. Struct.*, **5**(2), 196.
- Majumder, M., Gangopadhyay, T.K., Chakraborty, A.K., Dasgupta, K. and Bhattacharya, D.K. (2008), "Fibre Bragg gratings in structural health monitoring—Present status and applications", *Sensor. Actuat. A – Phys.*, **147**(1), 150-164.
- Myung, H., Wang, Y., Kang, S.C.J. and Chen, X. (2014), "Survey on robotics and automation technologies for civil infrastructure", *Smart Struct. Syst.*, **13**(6), 891-899.
- Pang, C., Yu, M., Gupta, A.K. and Bryden, K.M. (2013), "Investigation of smart multifunctional optical sensor platform and its application in optical sensor networks", *Smart Struct. Syst.*, **12**(1), 23-39.
- Talebinejad, I., Fischer, C. and Ansari, F. (2009), "Serially multiplexed FBG accelerometer for structural health monitoring of bridges", *Smart Struct. Syst.*, **5**(4), 345-355.
- Vasil'ev, S.A., Medvedkov, O.I., Korolev, I.G.E., Bozhkov, A.S., Kurkov, A.S. and Dianov, E.M. (2005), "Fibre gratings and their applications", *Quantum Electron.*, **35**(12), 1085.
- Zhang, P., Cerecedo-Nua, H.H., Qi, B., Pickrell, G. and Wang, A. (2003), "Optical time-domain reflectometry interrogation of multiplexing low-reflectance Bragg-grating-based sensor system", *Opt. Eng.*, **42**(6), 1597-1603.
- Zou, X.T., Chao, A., Wu, N., Tian, Y., Yu, T.Y. and Wang, X. (2013), "A novel Fabry-Perot fiber optic temperature sensor for early age hydration heat study in Portland cement concrete", *Smart Struct. Syst.*, **12**(1), 41-54.

HJ